Annals of Biomedical Engineering, Vol. 7, pp. 135–166, 1979 0191–5549/79/020135–37$02.00/0

A MODEL OF OVERALL REGULATION OF BODY FLUIDS

Noriaki Ikeda
Fumiaki Marumo
Masuo Shirataka
and
Toshiro Sato

Department of Information Sciences, Internal Medicine, and Physiology,
School of Medicine, Kitasato University, Kanagawa, Japan

A large-scale model of body fluid regulation was presented for the purpose of studying problems concerning body fluid disturbances and fluid therapy. This model, containing subsystems of circulation, respiration, renal function, and intra and extracellular fluid spaces, was described mathematically as a set of non-linear differential and algebraic equations of more than 200 variables. A special feature is that the respiratory and renal subsystems are combined into one system, so that acid-base disturbances of body fluid can be simulated over a wide range of time scales. Behavior of the model for various kinds of inputs simulated with a digital computer was in good agreement with a number of experimental results pertaining to body fluid and acid-base disorders. The model presented in this paper is considered to have good applicability to some clinical problems and to be a useful framework for physiological experimental research.

INTRODUCTION

A great number of clinical and experimental results have been accumulated on the physiological mechanisms of circulation, respiration, renal function, and acid-base balance in the human body, and many models have been proposed. It would be interesting to know if various clinical findings or measurements are reproduced or explained by a total biological system model designed on the basis of these individual subsystems.

One of the most important works in this field is that of Guyton et al. (16), who constructed an overall circulatory model for the purpose of revealing the causes of hypertension. In their model, the circulatory system and its

The authors gratefully acknowledge Dr. Arthur C. Guyton for kindly giving the information and answering some technical questions about his model, and Dr. Ronald White and Dr. D. G. Fitzjerrell for sending the technical reports and manuals.

Requests for reprints may be sent to Noriaki Ikeda, Department of Information Sciences, School of Medicine, Kitasato University, Kitasato 1-15-1, Sagamihara, Kanagawa, 228, Japan.

regulatory mechanisms were so accurately designed as to cover phenomena as brief as several seconds in duration.

We have been studying a systems approach to the diagnosis and therapy of body fluid and acid-base disorders. The purpose of this study is to provide a biological system model having a necessary and sufficient ability to accomplish this purpose, and to show its applicability to some clinical problems. Along these lines we have designed a comprehensive model with the following features: It contains subsystems of circulation, respiration, body fluids, renal function, and acid-base balance. The circulatory subsystem, which was complex in Guyton's model, is simplified so as to give steady-state values by neglecting rapid transients such as autoregulation or stress relaxation. The respiratory subsystem, which is required by the acid-base balance subsystem, was derived from the detailed model given by Grodins et al. (12, 13). Renal function, which was relatively simple in Guyton's model (16), is presented in detail, as well as the acid-base balance subsystem. In setting the parameter values, we used experimental results from the literature and some of our supplementary experiments.

Detailed explanations are given for each block of the model, followed by simulated responses to various inputs. These are compared with experimental data about body fluid and acid-base disturbances from the literature. Examples are shown of the application to clinical problems in the diagnosis and therapy of body fluid balance, and the possibilities for simulating some pathological states by this model are discussed. Several physiological problems to be resolved experimentally have emerged from the modeling. Finally, a proposal is made on a generalized approach to the use of modeling in medical investigation, such as standardization of symbols and expressions.

DESCRIPTION OF THE MODEL

The whole model consists of seven blocks as illustrated in Figure 1. Each block has input variables from the other blocks on the left side, output variables to the other blocks on the right, and on the top and bottom are the constant parameters and the inputs and outputs which are independent of the other blocks. This partition was made so as to make the interaction between blocks minimal, although some exceptions were permitted for convenience. These seven blocks are classified into three categories: the circulation and body fluids consisting of Blocks 1, 3, and 4; respiration containing Block 2 only; and renal function consisting of Blocks 5, 6, and 7.

All the variables in the model are abbreviated by up to four capital letters, and the attribute can easily be known from the first letter; for instance, P for pressure, V for volume, X for concentration, etc., with some exceptions of commonly used physiological terms such as GFR, HT, STBC, ADH, and ALD. These rules are given in Appendix I, with the definition and normal values of all the variables. Symbols for circuit representations used in the following

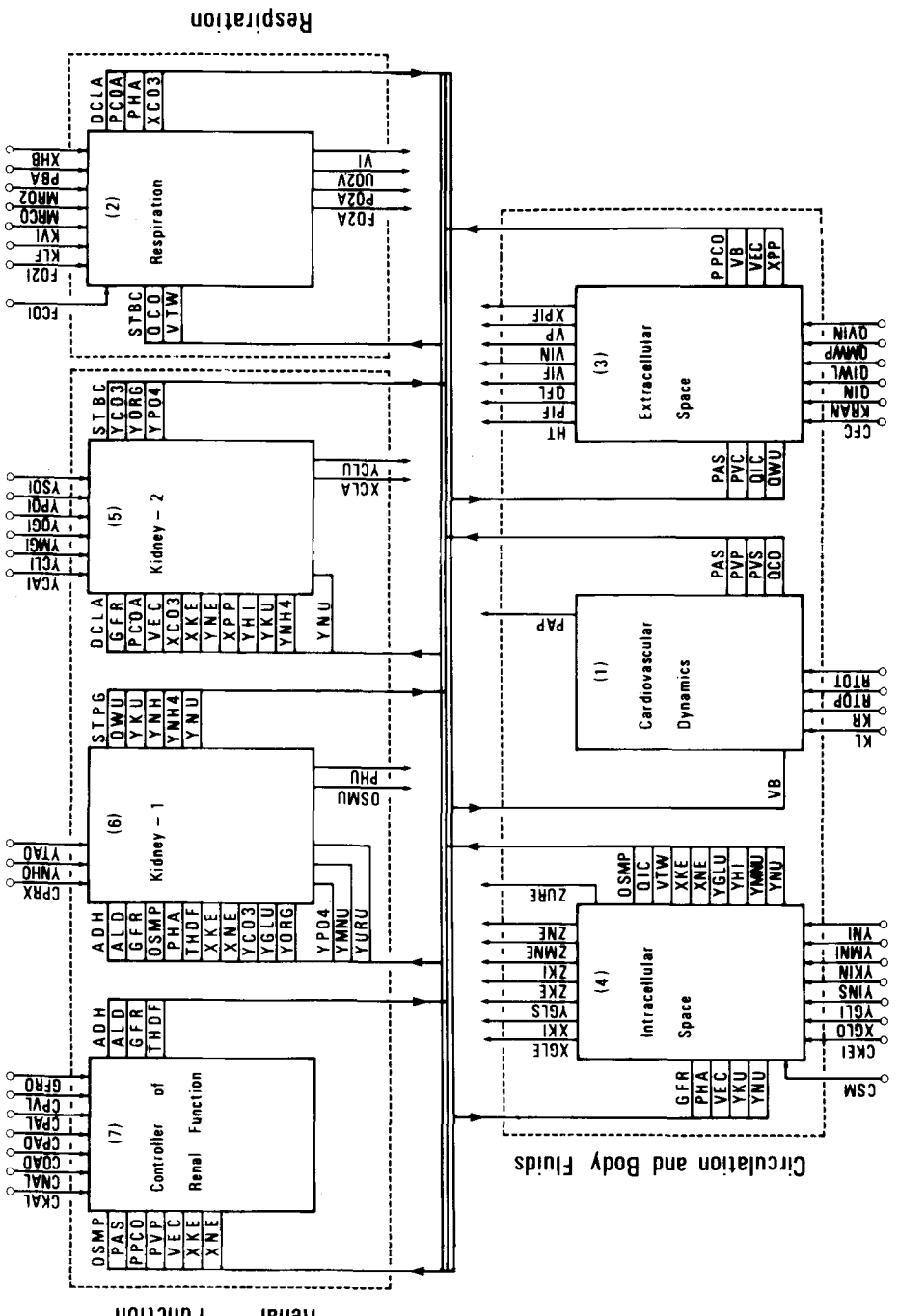

FIGURE 1. Block diagram of the model. Variables on the right side of each block indicate the outputs to the other blocks, and on the left, inputs from the other blocks. On the top and bottom of each block are fixed inputs or constant parameters (○——|) and the outputs which do not affect the other blocks (|——●). Explanations of the variables and their normal values are given in Appendix I.

paragraphs are in Appendix II, and detailed descriptions of the functions appearing in each block as F are in Appendix III.

The model assumes a healthy human male of approximately 55 kg in weight, the parameter values under standard conditions being average ones found in the literature.

1. Cardiovascular System (Block 1, Figure 2)

In Block 1, cardiac output (QCO) and the mean pressures in systemic arteries (PAS), systemic veins (PVS), the pulmonary artery (PAP), and pulmonary veins (PVP) are calculated from the circulatory blood volume (VB) on the basis of linear approximation of the Starling mechanism. This block gives the steady-state values of these variables after the system has settled from the transient state of local autoregulation or stress relaxation. This part of the model is based on the results of Grodins et al. (15) and Sato et al. (31), who analyzed systemic circulation as a network model and gave the relationships:

$$PAS = k_1\ QCO + k_2$$
$$PVS = k_3\ QCO + k_4$$
$$PAP = k_5\ QCO + k_6$$
$$PVP = k_7\ QCO + k_8$$

$$QCO = \frac{(VB - V_0) - (PVS0 \cdot \Sigma C_{si} + PVP0 \cdot \Sigma C_{pi})}{\sum_s TC_v + \sum_p TC_v + \frac{\Sigma CP_i}{KL} + \frac{\Sigma C_{si}}{KR}},$$

where k's are regression constants, ΣC_{si} and ΣC_{pi} are total compliances of systemic and pulmonary circulation, $\sum_s TC_v$ and $\sum_p TC_v$ are time constants of systemic and pulmonary veins, respectively, and V_0 is the unstressed volume. The parameter values were determined from experimental data (15, 31). From these equations all the variables of this block are given as a linear function of VB. Some of the parameter values were readjusted slightly on the basis of results of our supplementary experiment. We might choose a more complex dynamic model of the cardiovascular system, but such a choice would make it difficult to simulate long-term behavior of the body fluids.

Function F11 or the parameters HF0 through HF4 may be used to simulate some abnormal states of the heart, e.g., to reproduce a heart failure by reducing the slope of the venous return curve by setting KR at a lower value and HF's to appropriate values. However, the present paper is concerned only with modeling normal function.

2. Respiratory System (Block 2, Figure 3)

Block 2 is related to the controlling and the controlled systems of respiration, and the acid-base balance in blood. The controlling system is given by

the function F21 by which the steady-state value of alveolar ventilation (VI) is calculated as a function of pH, Pco_2, and Po_2 in blood:

$$VI = VR \cdot VI_0, \tag{1}$$

$$VR = k_1 [H^+] + k_2(k_3+k_4/(Po_2-c)\,(Pco_2+k_5)+k_6, \tag{2}$$

where VI_0 is the normal value of VI, and VR is the ventilation ratio. The values of the coefficients, k_i, are given in Appendix III. Eq. (2) is Gray's regression formula (11) modified by Cunningham et al. (6). The parameter values are determined from recent experimental results (5, 8, 18, 20, 25, 26), with some additional corrections to prevent the numerical solution from diverging in the case of alkalosis or hypercapnia. Plots of VR values against the independent change in pH, Pco_2, or Po_2 are shown in Figure 4.

The controlled system (plant) or respiration is in the upper and the lower part of this block. The former gives the dynamics of concentration and partial pressure of CO_2 with the input to and the output from the blood. The latter denotes the corresponding mechanisms for O_2. The following relations are assumed for the partial pressures of CO_2 and O_2 in alveoli

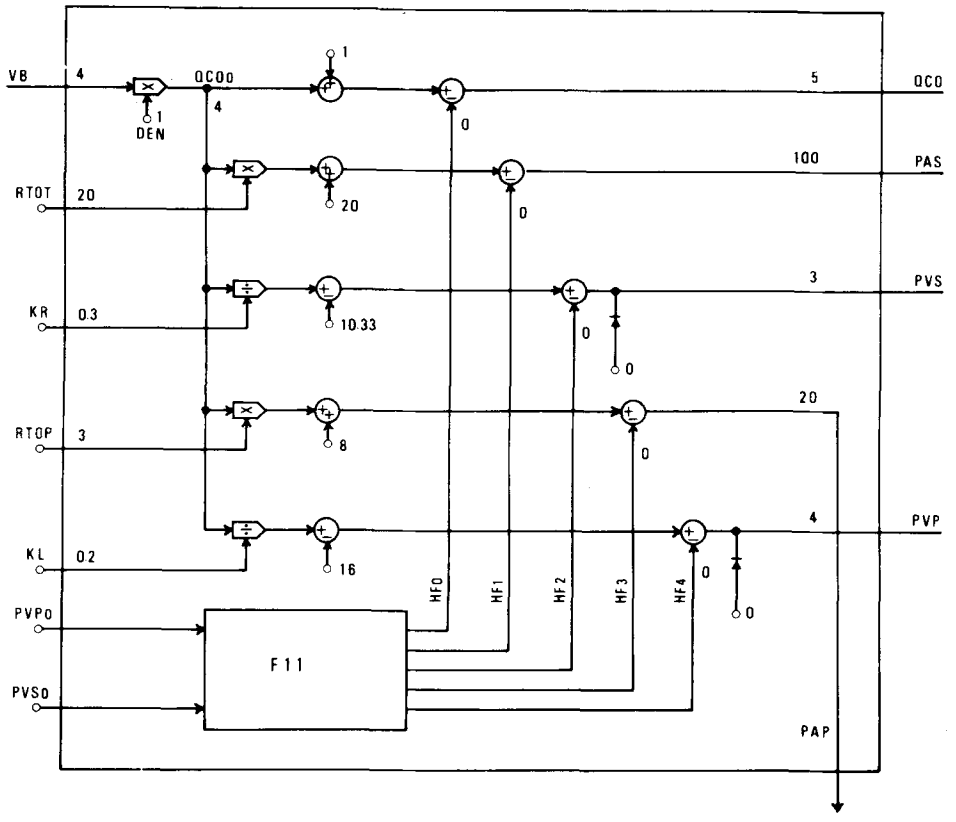

FIGURE 2. Block 1. Cardiovascular system: blood pressure, cardiac output and venous return.

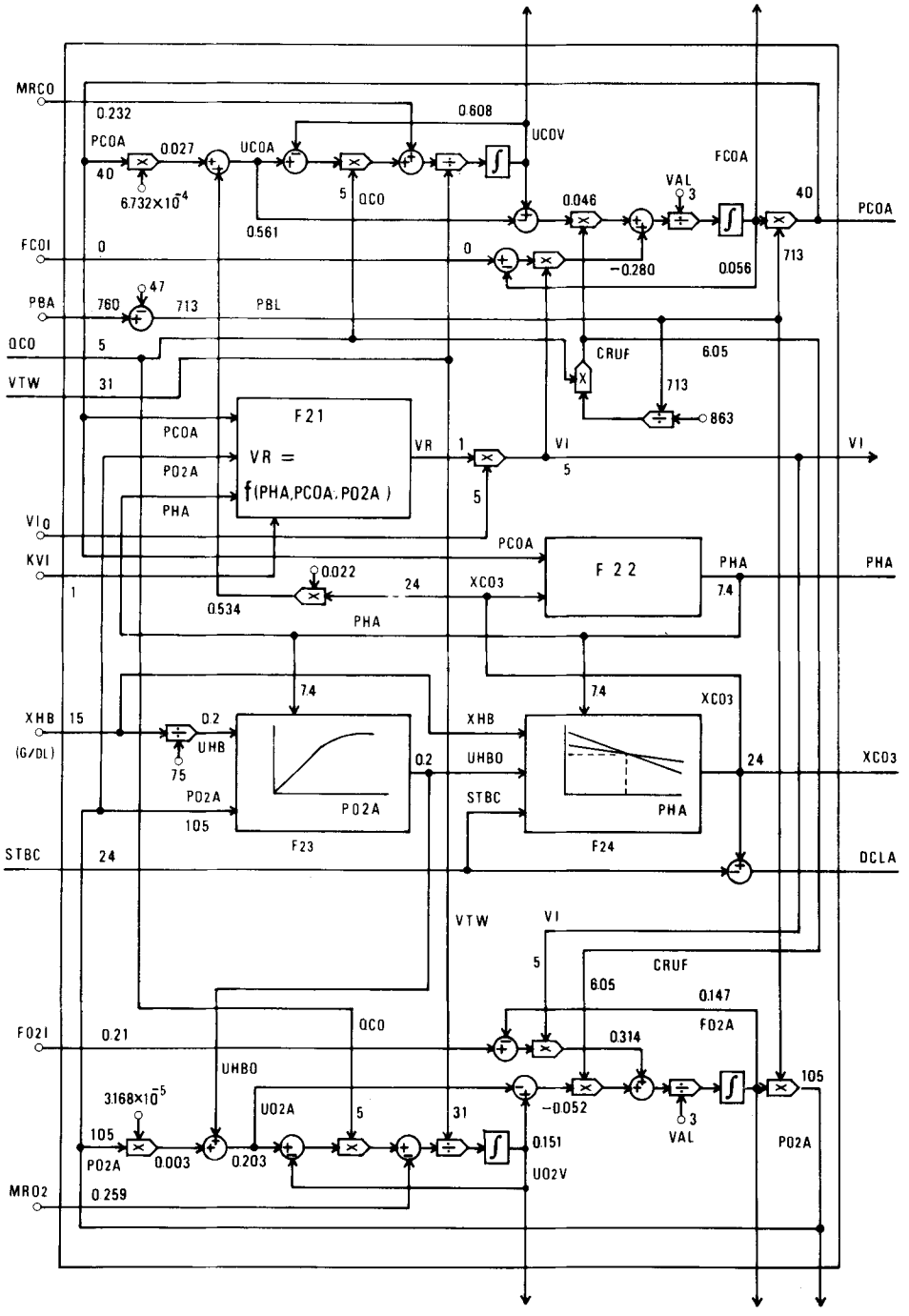

FIGURE 3. Block 2. Respiratory system (respiratory acid-base balance): pH, Pco_2, Po_2, and the buffer line.

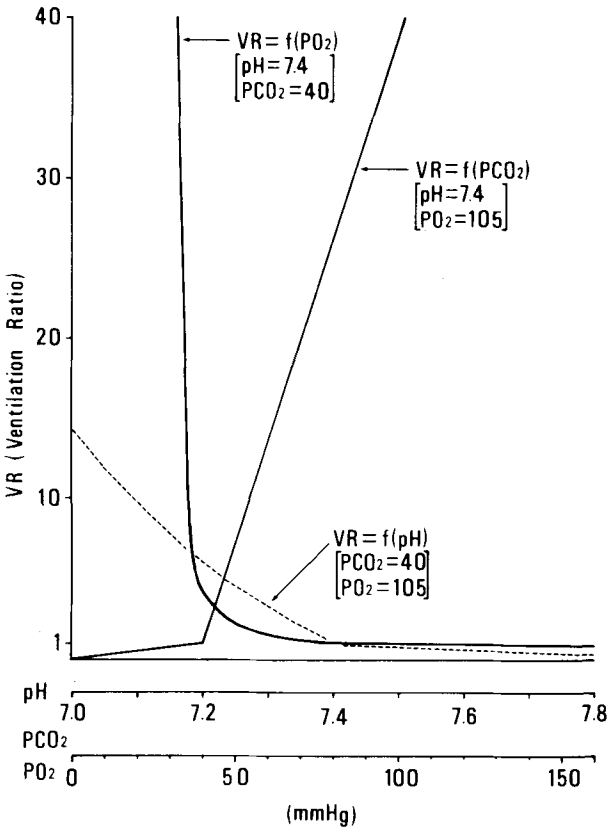

FIGURE 4. Curves of the ventilation ratio (VR used in the model as a function of pH, Pco_2, and Po_2 (F21 in Block 2).

(FCOA and FO2A), the concentrations of CO_2 and O_2 in arterial blood (UCOA and UO2A) and in venous blood (UCOV and UO2V), and the partial pressures of CO_2 and O_2 in arterial blood (PCOA and PO2A):

$$\begin{aligned} \text{d (FCOA) /dt} &= \text{(VI (FCOI–FCOA) + 863/ (PBA–47)} \\ &\quad \text{x QCO (UCOV–UCOA)) /VAL} \end{aligned} \tag{3}$$

$$\begin{aligned} \text{d (FO2A) /dt} &= \text{(VI (FO2I–FO2A) + 863/ (PBA–47)} \\ &\quad \text{x QCO (UO2V–UO2A)) /VAL} \end{aligned} \tag{4}$$

$$\text{d (UCOV) /dt} = \text{(MRCO + QCO (UCOA–UCOV)) /VTW} \tag{5}$$

$$\text{d (UO2V) /dt} = \text{(MRO2 + QCO (UO2A–UO2V)) /VTW} \tag{6}$$

$$\text{UCOA} = 6.732 \cdot 10^{-4}\ \text{PCOA} + 0.022\ \text{XCO3} \tag{7}$$

$$\text{UO2A} = 3.168 \cdot 10^{-5}\ \text{PO2A} + \text{UHBO.} \tag{8}$$

Function F22, F23 and F24 constitute the blood buffer system. F22 is the Henderson-Hasselbalch equation:

$$\text{PHA} = 6.1 + \log\ (\text{XCO3/ (0.03 PCOA)}). \tag{9}$$

F23 is an oxygen saturation curve, and F24 is an in vivo CO_2 dissociation curve (3). The hemoglobin buffer system, the Bohr effect, and the Haldane effect are thus taken into account in the model.

3. Extracellular Space (Block 3, Figure 5)

Block 3 deals with water intake and output, the distribution of extracellular fluid (ECF) consisting of plasma (PF) and interstitial fluid (ISF), and protein flow. Water input to plasma (increase in PF) is given by:

$$\begin{aligned} Vp^{+} = {} & \text{intake by mouth (QIN)} + \text{intravenous infusion (QVIN)} \\ & + \text{metabolic water production (QMWP)} \\ & + \text{lymphatic inflow (QLF)}, \end{aligned} \tag{10}$$

and the output from plasma (decrease in PF) is:

$$\begin{aligned} Vp^{-} = {} & \text{insensible water loss (QIWL)} + \text{urine (QWU)} \\ & + \text{outflow from capillary (QCFR)}; \end{aligned} \tag{11}$$

therefore, the change in plasma volume is given by:

$$d(VP)/dt = Vp^{+} - Vp^{-}. \tag{12}$$

Net transcapillary filtration of fluid (QCFR) from PF to ISF is given by:

$$\begin{aligned} QCFR = {} & \text{capillary filtration coefficient (CFC)} \\ & \times \text{filtration pressure (PF)}, \end{aligned} \tag{13}$$

where the filtration pressure (PF) is determined by the opposing forces of hydrostatic pressures (PC and PIF) and oncotic pressures (PPCO and PICO) across the capillary membrane:

$$Pf = PC - PPCO - PIF + PICO. \tag{14}$$

The lymphatic flow rate (QLF) is determined by F32 as a function of ISF pressure (PIF), which is given in turn by F31 as a function of ISF volume (VIF). Both of these functions are from the experimental data of Guyton et al. (17, 28, 37).

The lower part of Block 3 represents the dynamics of proteins in plasma and interstitial fluid. It is assumed that the protein flow from plasma into ISF (YPLC) is proportional to the function F33 of capillary pressure (PC), and that the decrease in interstitial protein (YPLF) is proportional to the lymphatic flow rate (QLF). Also, the movement of protein into interstitial gel space and the construction or destruction of protein in the liver are contained in the model, simply using the transfer function derived from Guyton's model (16).

4. Intracellular Space and Electrolytes (Block 4, Figure 6)

Block 4 deals with the dynamics of intracellular fluid volume, osmotically active substances of body fluid, and intracellular acid-base balance. The os-

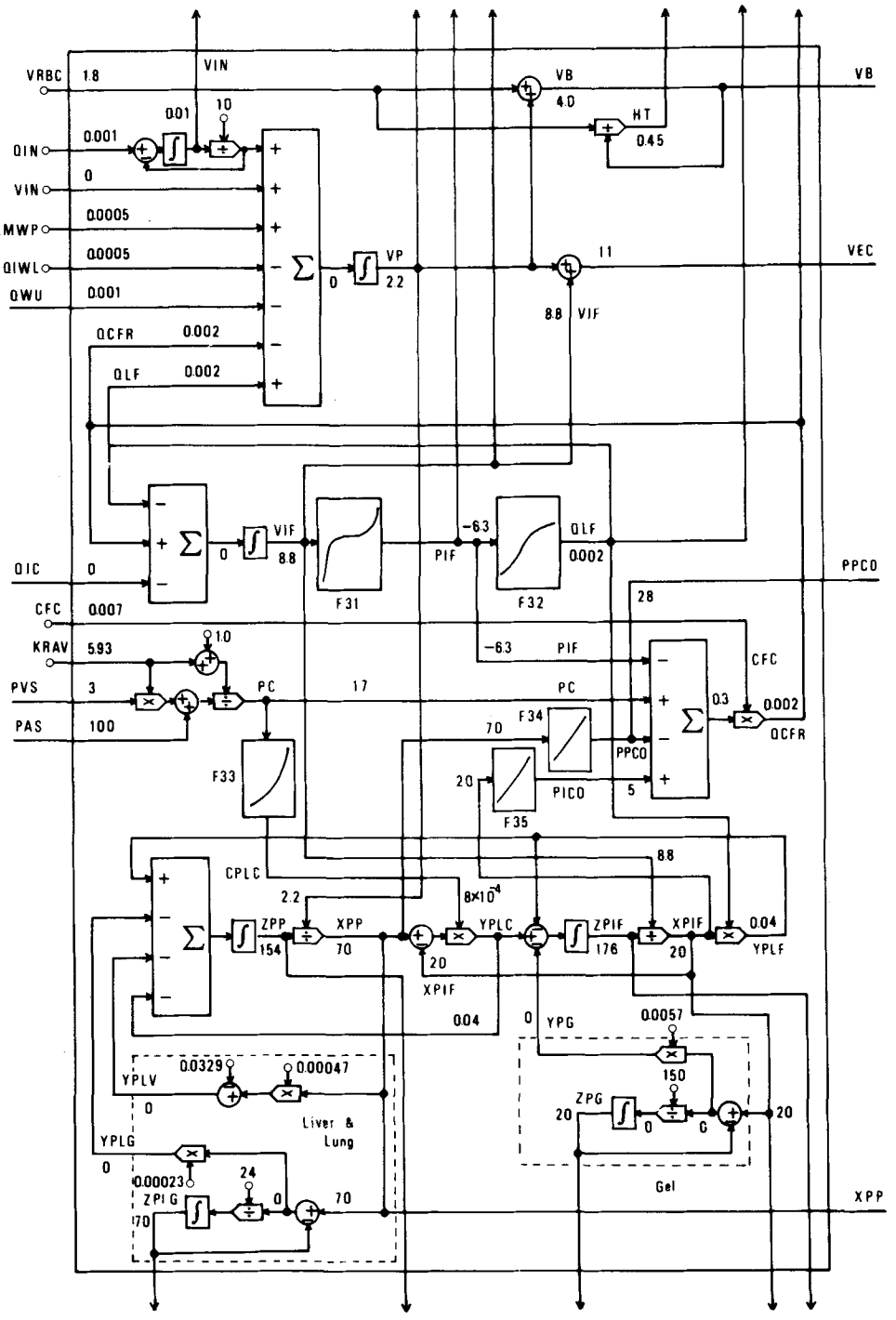

FIGURE 5. Block 3. Extracellular space: capillary, lymphatic vessels, and interstitial fluid.

motically active substances of the body fluid are Na, K, glucose, urea, and mannitol. The change in ECF sodium content (ZNE) is given by:

$$\begin{aligned} d(ZNE)/dt = {} & \text{intake of Na (YNIN)} - \text{excretion of Na (YNU)} \\ & + \text{increase in Na exchanged with the } H^+ \\ & \text{transferred into ICF.} \end{aligned} \tag{15}$$

The change in ECF potassium content (ZKE) is similarly given by:

$$\begin{aligned} d(ZKE)/dt = {} & \text{intake of K (YKIN)} - \text{excretion of K (YKU)} \\ & + \text{transmembrane K shift exchanged with the} \\ & H^+ \text{ transferred into ICF} \\ & - \text{transfer into ICF accompanying the secretion} \\ & \text{of insulin in the metabolism of glucose,} \end{aligned} \tag{16}$$

the third term of which is given by F41 formulated from experimental data on the effect of pH on potassium metabolism (4, 29). The fourth term in Eq. (14) which is given as the middle part of this block represents the mechanism for glucose metabolism and secretion of insulin. The behavioral characteristics of glucose metabolism are determined by the parameters, CGL1, CGL2, and CGL3. Metabolic disorders of glucose may be modeled by changing the value of these parameters appropriately. Function F42 represents the Tm-limited reabsorptive mechanism for glucose (24).

In the lowest part of this block are the input and output of urea and mannitol. As the reabsorption of urea is passive (24), it is assumed that approximately 60% of the filtered load is finally excreted. Mannitol, which is normally negligible in the body, is contained in the model because it is often used for therapy. Plasma osmolality (OSMP) is determined by the concentration of sodium, potassium, glucose, urea and mannitol. A model for the intracellular buffering mechanism was devised only for explaining the findings in experimental metabolic acidosis and alkalosis (10, 24, 34) because of a lack of detailed quantitative experiments.

5. Kidney (2) (Block 5, Figure 7)

In this block the renal excretion rate is given for bicarbonate, calcium, magnesium, phosphate, and organic acids, according to the Tm-limited mechanism for reabsorption (24), by the functions F51 – F56 respectively. Since the reabsorption of chloride is assumed to be passive against Na^+, K^+, etc., the renal excretion rate of chloride is calculated as the difference of the excretion rate of the cations and anions other than chloride. Standard bicarbonate at pH = 7.4 (STBC) is defined as the difference of the ECF concentration of cations and anions other than bicarbonate. The excretion rate of bicarbonate (YCO3) is affected by the P_{CO_2} in arterial blood via the function F50 (27).

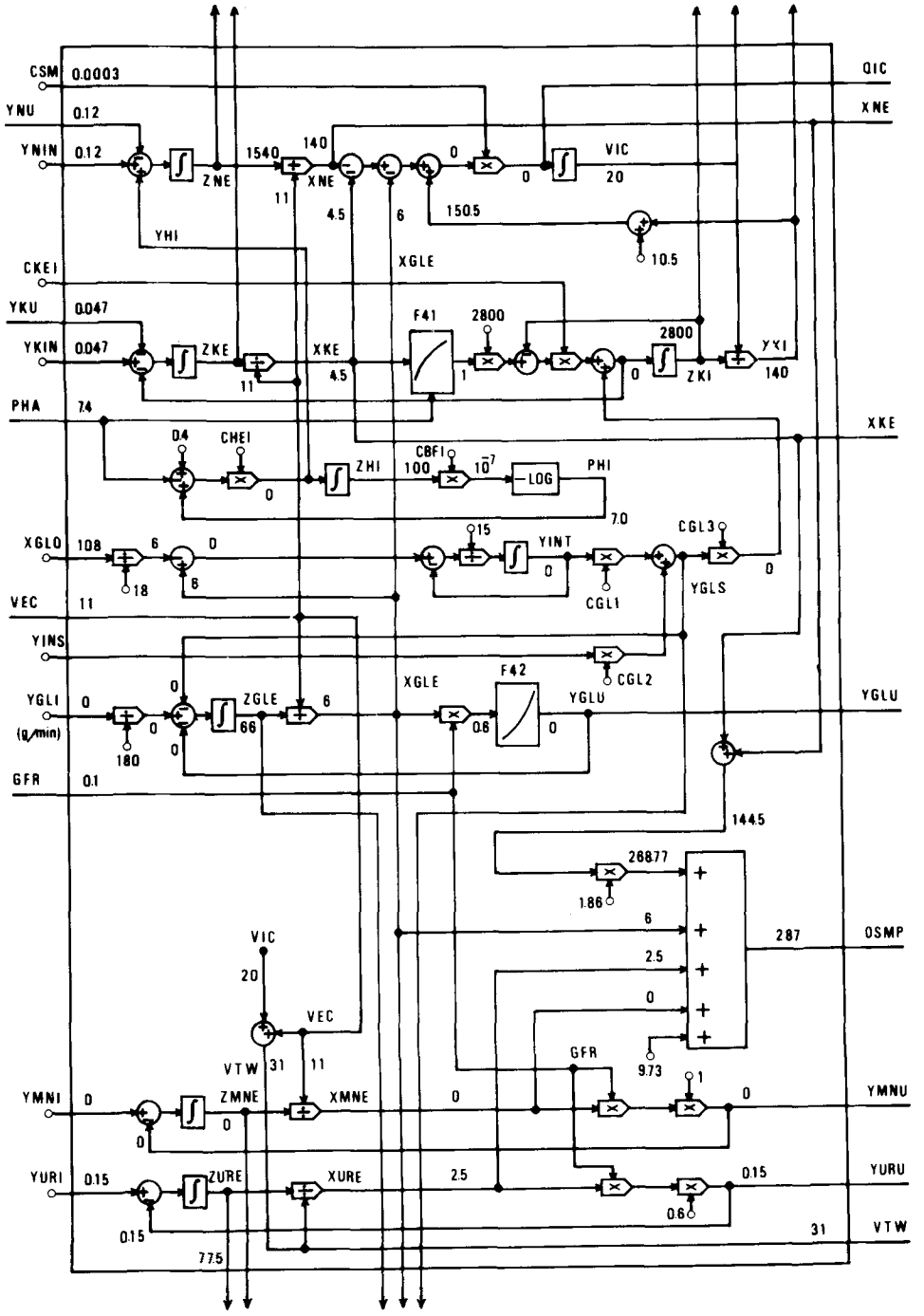

FIGURE 6. Block 4. Intracellular space and electrolytes: concentrations of sodium, potassium, glucose, urea, and mannitol, plasma osmolarity and intracellular buffer.

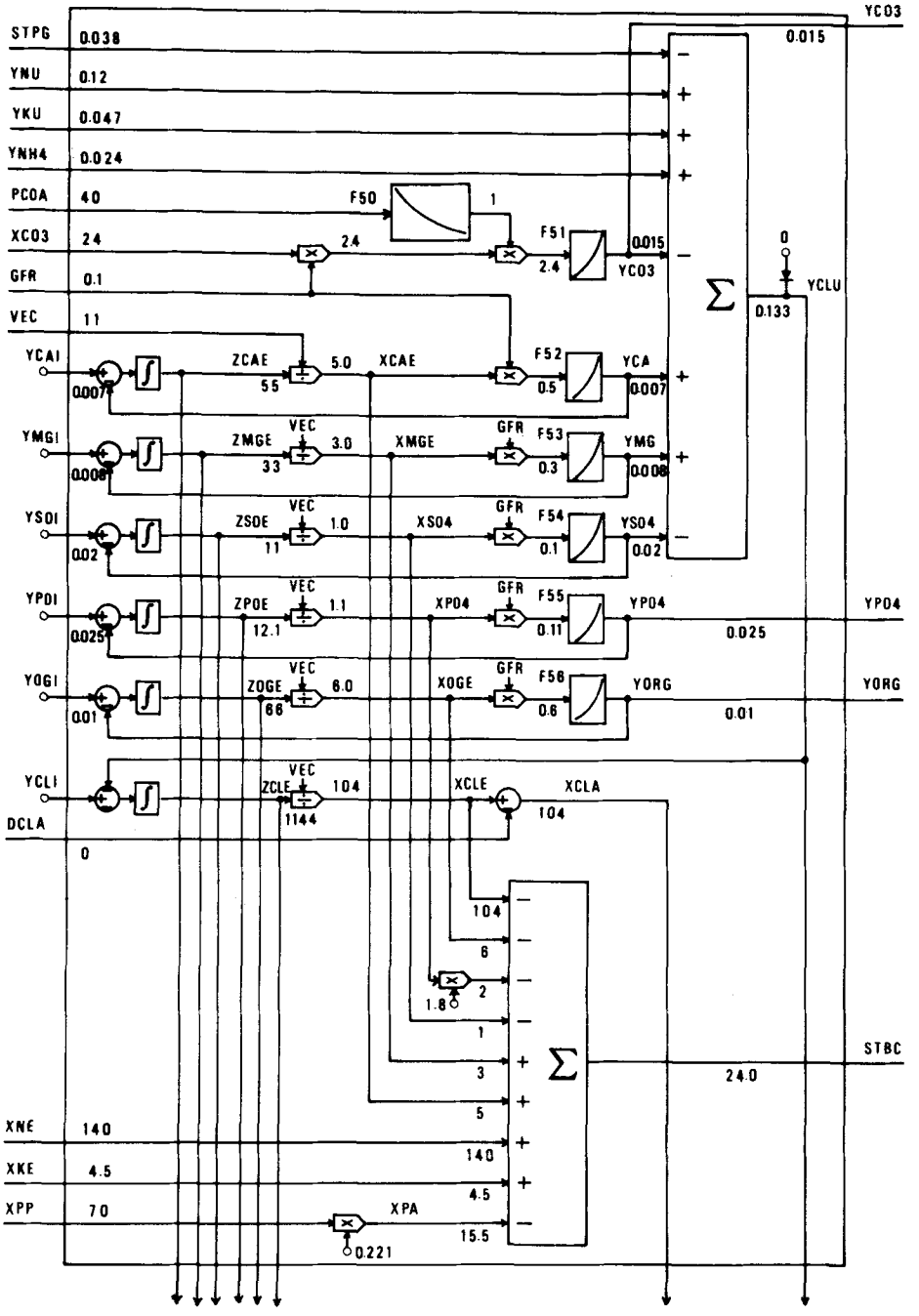

FIGURE 7. Block 5. Kidney (2) (metabolic acid-base balance): standard bicarbonate, urinary excretion of chloride, calcium, magnesium, bicarbonate, sulphate, phosphate, and organic acid.

6. Kidney (1) (Block 6, Figure 8)

The upper part of Block 6 is the main part of the kidney which involves the reabsorption and excretion of water, sodium, and potassium. It is assumed that 80% of the glomerular filtration rate (GFR) is reabsorbed in the proximal tubule under normal conditions. The proximal reabsorption is modified by the variable THDF as described below. As the reabsorption of water is assumed to be iso-osmotic down to the distal tubule, rate of water flow in the distal tubule is determined by dividing the sum of the excretion rate of Na, K, glucose, urea, and mannitol, by the plasma osmolality. The mechanism of the increase in urine osmolality caused by the reabsorption of water by ADH is modeled as a lumped parameter system. Aldosterone is assumed to operate on the distal tubule, and to increase the sodium reabsorption and interchangeably decrease the potassium reabsorption, and to increase the excretion rate of titratable acid (YTA), by which the alkalosis of hyperaldosteronism could be brought about. Thus, the urine output (QWU) and the renal excretion rates of sodium (YNU) and potassium (YKU) are determined. The urine osmolality is calculated from the excretion rates of Na, K, glucose, urea and mannitol already given in Block 4.

In the lower part of the block, the urine pH and the excretion rate of ammonia (YNH4) and titratable acid (YTA) is determined. The excretion of ammonia is subject to the influence of the urine pH (PHU) with a relatively large time constant (24) which is given by F61. The excretion of titratable acid increases with a decrease in the blood pH (PHA) and is lowered with an extreme decrease in the urine pH, on which, however, satisfactory data are lacking. F64 and F65 are the functions for calculating the urine pH from the excretion rates of phosphate (pK = 6.8), and organic acids (avs pK = 4.3), and the Henderson-Hasselbalch equation. The excretion of ammonia and titratable acid facilitates sparing of sodium which is reabsorbed in exchange for those ions.

7. Controller of the Renal Function (Block 7, Figure 9)

This block gives the glomerular filtration rate (GFR) and the three control signals which operate on Block 6, antidiuretic hormone (ADH), aldosterone (ALD), and the effect of volume expansion or pressure diuresis (THDF). All values of the above are taken as a ratio to the normal level. GFR is a sigmoid-shaped function of arterial pressure representing the autoregulatory mechanism given by the function F74 (1) and is controlled by the change in ECF volume (VEC) through the volume receptor. Secretion of ADH is assumed to be driven by the weighted sum of the signals from the volume receptors and the osmoreceptors. Secretion of aldosterone via the renin-angiotensin system is assumed to be related to ECF potassium concentration, tubular sodium concentration, arterial pressure, and volume receptor signals. We are not interested here in the detailed mechanism of the renin-angiotensin-aldosterone system, but only in the transfer function between input and output of the

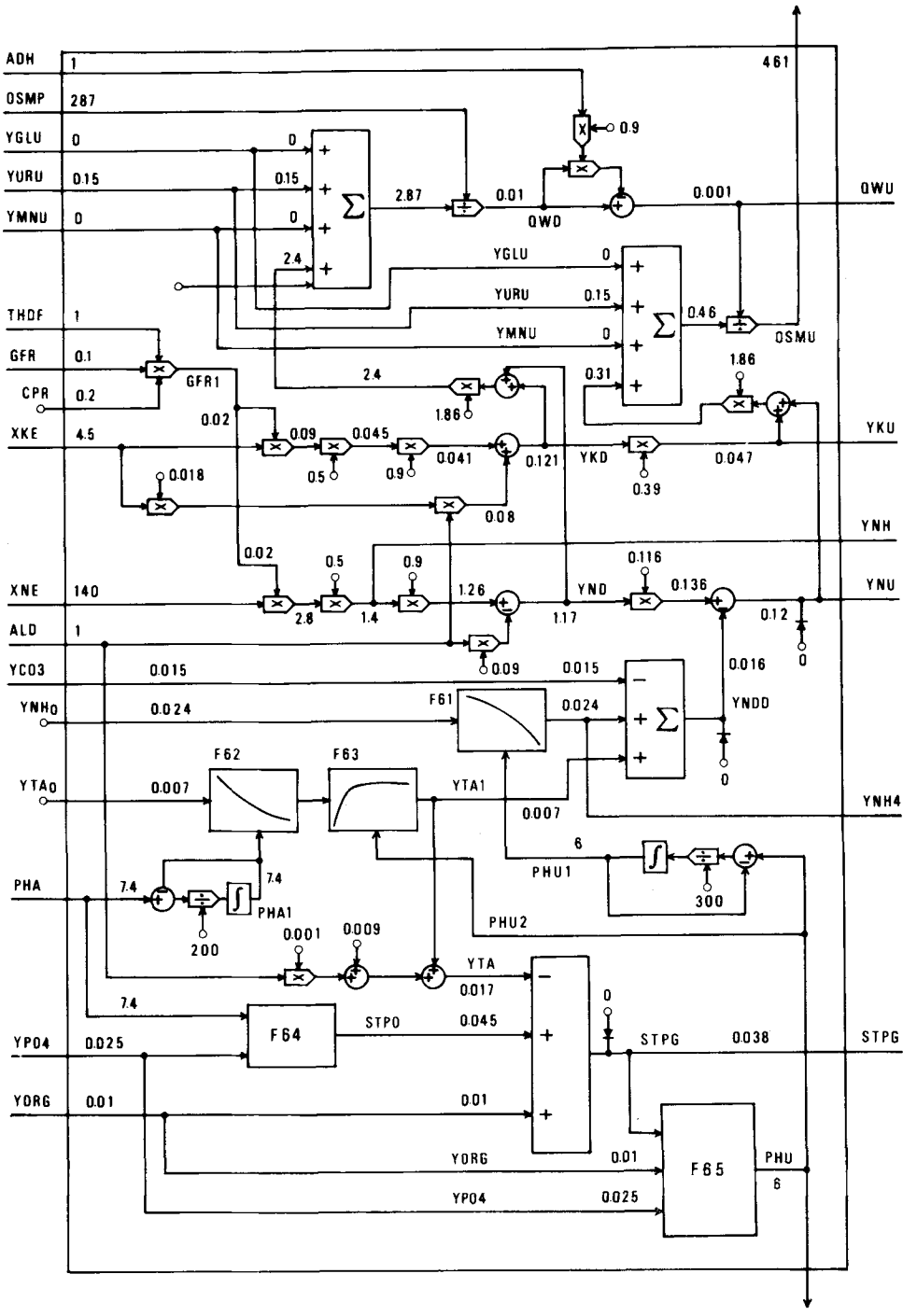

FIGURE 8. Block 6. Kidney (1): urinary excretion of water, sodium, potassium, ammonia, and titratable acid, and pH of urine.

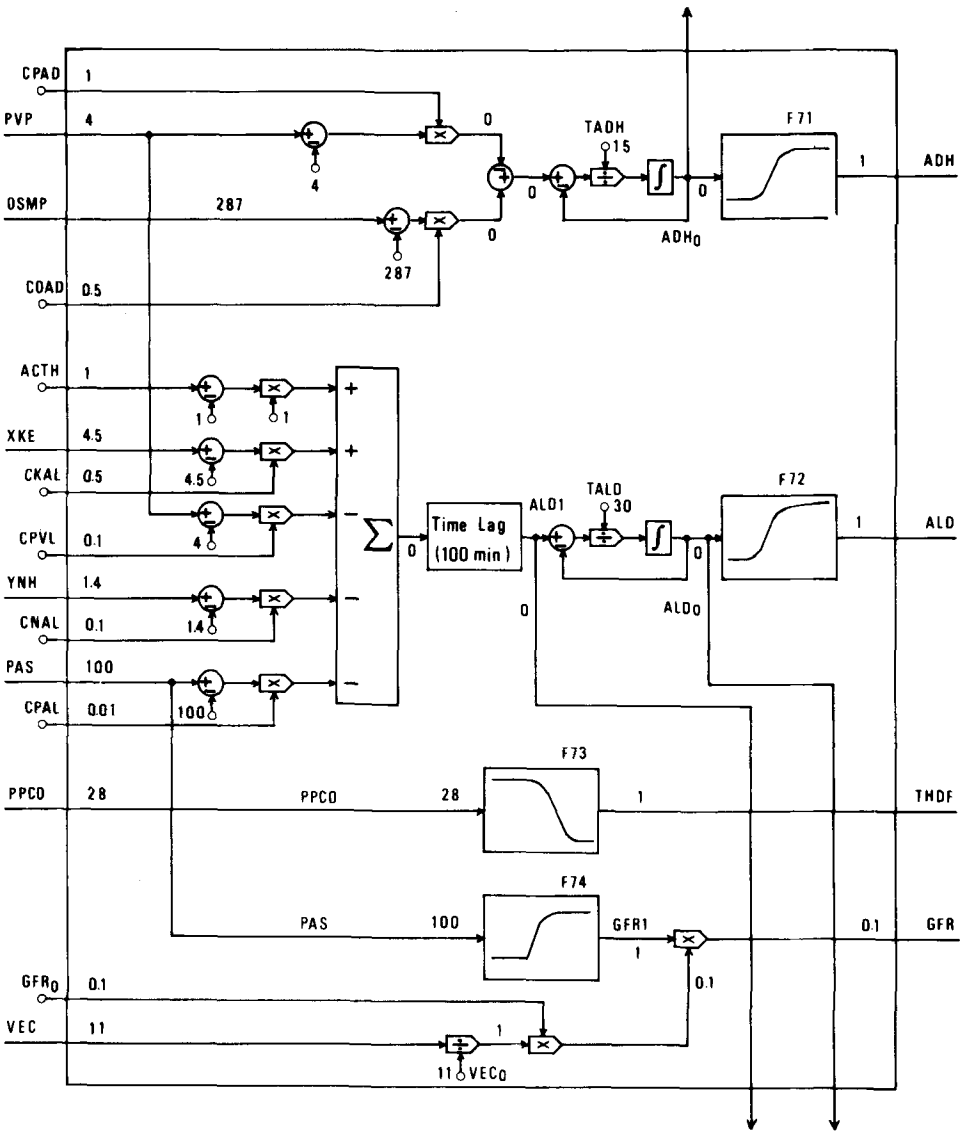

FIGURE 9. Block 7. Controller of renal function: antidiuretic hormone, aldosterone, THDF, and GFR.

subsystem. The values of weighting coefficients and of time constants were determined by reference to the literature (2, 33), and from simulations of water loading or saline infusion. We feel, however, that these parameter values should be refined through further experiments.

The variable THDF is intended to represent the effect of body fluid volume expansion on increased urinary output (saline diuresis, for example) which could not be fully explained only by ADH and ALD, and which seems to be one of the most significant functions of the model. While a number of different theories have been advanced, we have assumed it to act via the effect of plasma oncotic pressure on the reabsorption rate in the proximal tubule, given by the function F73 based on the experimental data (22).

COMPUTER SIMULATION OF THE MODEL

The model, written in Fortran IV language, was executed on a HP-21MX mini-computer with 64 KB of memory and the real time operating system, RTE-II. The time step for computation was set at 1.0 second, which made the simulation speed fifteen times as fast as real time when all the blocks were included. This speed is too low to achieve a long-term simulation of several months. The minimum time step was determined by that of the respiration block (Block 2) whose frequency characteristics were about ten times as rapid as those of the other blocks. Simplification of the respiratory block will be necessary for reducing the computation time.

COMPARISON OF THE MODEL BEHAVIOR WITH EXPERIMENTAL DATA

In this section we compare the results of simulation and the experimental data.

1. Water Loading and Saline Infusion

Water loading is one of the most fundamental tests of the interaction between body fluids and the kidney. Figure 10 shows the simulation of oral water intake and of intravenous infusion of physiological saline at a rate of 1000 ml per 5 minutes. These kinds of experimental data are available in many studies (22, 24, 33). In the case of water intake, a marked increase in urine output was accompanied by a decrease in ADH caused by the reduced plasma osmolality (OSMP). In the case of physiological saline infusion, however, urine output did not increase except for the effect of THDF, and the elevated ECF volume did not return to normal for a number of hours. Dynamical property (gain and time constant) for ADH secretion was based mainly on the experimental analysis by Shimizu (33) who investigated macroscopic transfer characteristics from plasma osmolality to urine output; therefore, the time constant, TADH, in this model is not strictly the same as that of ADH secretion itself.

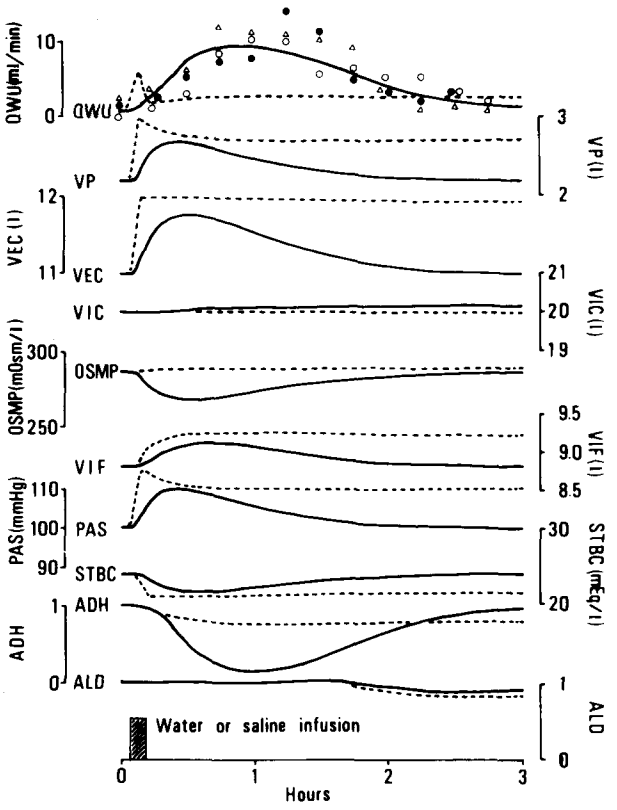

FIGURE 10. Simulation of acute water loading (————) and intravenous saline infusion (– – – – – –), both at a rate of 1000 ml per 5 minutes. Urine output (QWU) of three human subjects after intake of 1000 ml water in 5 minutes are also shown (○, ●, and △).

2. Respiratory Responses to Increased Pco_2 and Decreased Po_2

The transient response of the respiratory system to 5% CO_2 inhalation is shown in Figure 11. The model's predictions for the steady-state response of alveolar ventilation (VI) to increased CO_2 concentration and to decreased O_2 concentration in inspired air are presented in Table 1 and Table 2, respectively. The experimental data of Dripps and Comroe (7) and the values given by the Grodins' model (12) are tabulated together for comparison. Although our model is based on recent experimental results, the predictions of the model are generally similar to the early experiment or to the Grodins' model.

3. Glucose Metabolism and Potassium

The model includes glucose metabolism which plays an important role in fluid therapy. Figure 12 shows a test of glucose metabolism including the secretion of insulin with a concomitant decrease in ECF potassium concen-

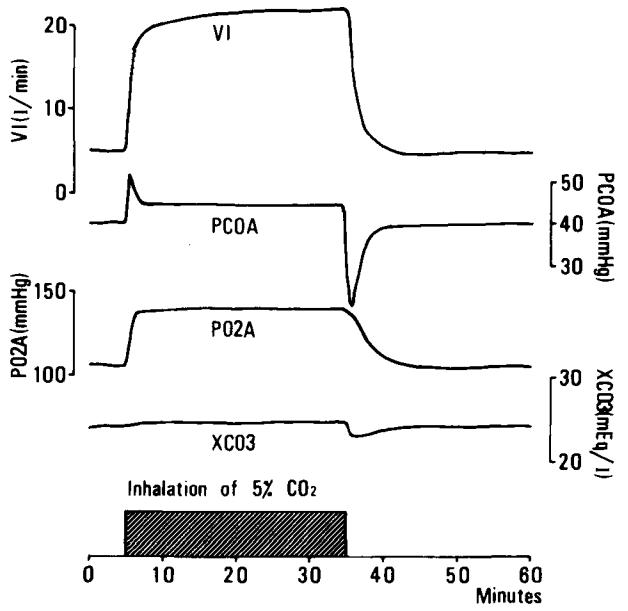

FIGURE 11. Simulation of the transient response of respiratory parameters to the inhalation of 5% CO_2 for 30 minutes.

tration. Dotted lines indicate clinical data (23) for oral ingestion of glucose, which is not exactly the same input condition as that of the simulation because the model does not include the gastrointestinal system.

4. Metabolic Acid-Base Disturbances and Intracellular Buffering

A comparison was made between simulation and experiment for the distribution and neutralization of infused acid or alkali in nephrectomized dogs (34, 35) (Tables 3 and 4). The value in parentheses indicates the estimated percentage of each buffering mechanism (24). The inputs to the model

TABLE 1
Steady State Values of Alveolar Ventilation for Various CO_2 Concentrations

Concentration of CO_2 in inspired air (%)	Alveolar ventilation (1/min) Experiment[a]	Grodins' model[b]	The present model
.03	4.6	–	5.0
1	5.6	6.10	6.0
2	6.6	7.67	7.5
4	11.3	14.11	14.0
5	22.5	–	21.9
6	–	29.70	35.2
7.6	47.9	–	67.8

[a]From Dripps and Comroe (7).
[b]From Grodins et al. (14).

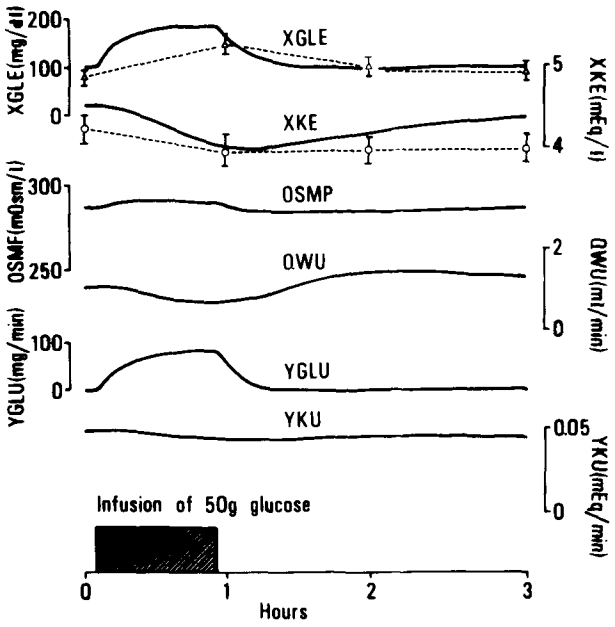

FIGURE 12. Simulation of the glucose tolerance curve with the ECF potassium concentration, and the experimental data (———△———) by Perez et al. (23).

corresponding to the infusion of acid or alkali were 300 mEq of chloride or 300 mEq of sodium respectively. In the computation, renal function (Blocks 6, 7, and most of Block 5 in the model) was eliminated to realize the same condition as in the experiment, and the value at an hour after infusion was used for comparison. The metabolic alkalosis was predicted well by the model, whereas the result of simulation of metabolic acidosis agreed less well with the experimental data. The latter descrepancy could have been due to asymmetry of the buffering mechanism of the body which was not included in the model.

TABLE 2
Steady State Values of Alveolar Ventilation for Various O_2 Concentrations

Concentration of O_2 in inspired air (%)	Alveolar ventilation (1/min)	
	Experiment[a]	The present model
20.93	4.9	5.0
18.0	4.9	5.3
16.0	5.4	5.6
12.0	5.4	6.9
10.0	6.2	8.8
8.0	10.4	13.4

[a]From Dripps and Comroe (7).

TABLE 3
Metabolic Acidosis and the Mechanism of Buffering

	$\dot{V}i$	P_{CO_2}	pH	Difference in total ECF stores (mEq) Na	K	HCO_3	Cl
Experiment[a]	–	–	7.10	+65	+28	−78	−10
				(36%)	(15%)	(43%)	(6%)
Simulation[b]	21.7	9.1	7.23	+44	+10	−223	−24
				(15%)	(3%)	(74%)	(8%)

[a]Infusion of 180 mEq of HCl into nephrectomized dogs.
[b]Input of 300 mEq of chloride with renal blocks bypassed.

5. Respiratory Acid-Base Disturbances and Compensation by the Kidney

In acid-base disturbances, the kidney plays a central role in the compensatory reactions of the body when the normal response of respiration does not occur. One of the features of our model is that it can predict that kind of phenomenon. The long-term time course of the model behavior in respiratory acidosis or alkalosis is depicted on a pH-[HCO_3] plane (Figure 13). Curve OA corresponds to the response to 10% CO_2 inhalation, and OB, the response to the hyperventilation in which VI was raised to three times normal. For about the first two hours the compensation for the disturbance was mainly due to intracellular buffering. After that, long-term renal compensation appeared. The time course on the pH-[HCO_3] diagram was in good agreement with the result given by Woodbury (38) who analyzed the experimental data of Giebisch et al. (10).

COMMENT ON CLINICAL APPLICATION

The model was designed originally for the purpose of simulating body fluid disorders, i.e., edema, dehydration, acid-base disturbances, and their fluid therapy. Fluid therapy is an important and quite ordinary therapeutic means, but many problems are left to be solved, e.g., what is the optimum therapy for a body fluid disturbance, or what kind of disorder is really

TABLE 4
Metabolic Alkalosis and the Mechanism of Buffering

	$\dot{V}i$	P_{CO_2}	pH	Difference in total ECF stores (mEq) Na	K	HCO_3	Cl
Experiment[a]	–	–	7.65	−115	+3	+228	+9
				(26%)	(–)	(66%)	(2%)
Simulation[b]	5.1	40.7	7.59	−80	−12	+178	+25
				(27%)	(4%)	(59%)	(8%)

[a]Infusion of 437 mEq of $NaHCO_3$ into nephrectomized dogs.
[b]Input of 300 mEq of sodium with renal blocks bypassed.

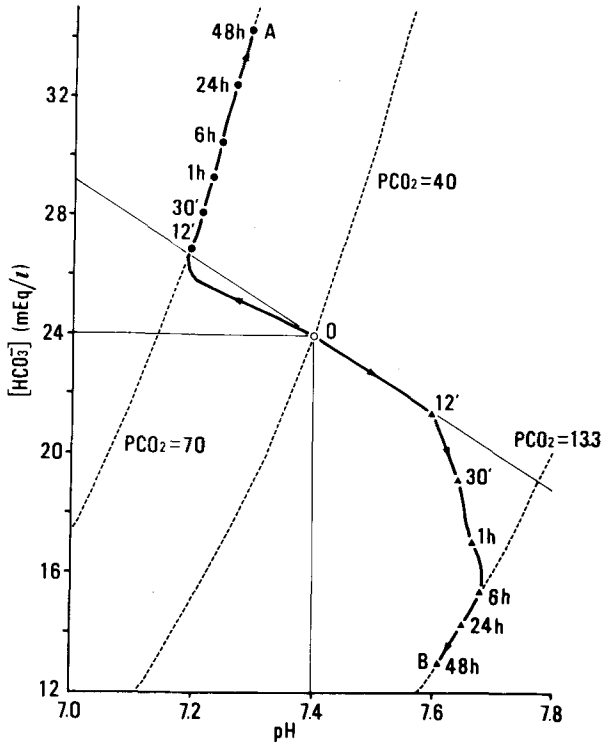

FIGURE 13. Simulation of respiratory acidosis and alkalosis with the renal compensation. Point O shows the normal value of the model of the pH–[HCO_3] plane. ——▲—— indicates the plotting of simulated response to 10% CO_2 inhalation for 48 hours, and ——●—— indicates that of hyperventilation in which VI was fixed at 15 1/min. Equi-pressure lines of Pco_2 are shown with dotted lines for the Pco_2 values of 13.3, 40.0, and 73.0 mmHg.

happening in the interior of the cells which are not accessible by usual techniques of clinical examination. The clinical problem in body fluid disorders has two stages. The first is the diagnostic stage; examining what is deficient or excessive and estimating how much it is. Various methods have been proposed for that purpose: For instance, the estimation of salt and water for different types of dehydration was discussed by Marriot (21). The second is the therapeutic stage. Various methods have been also proposed mainly on an empirical basis (21, 32). It may be desirable to use a "safety factor" of 1/2 or 1/3 to be multiplied by the estimated deficit at the actual treatment. Hypotonic solutions are considered less dangerous in fluid therapy in general (32). The model may be used to solve some of these problems, or at least to provide an interpretation of them.

For example, Figure 14 illustrates a simulation in which 4.5 liter of ECF was removed in 10 hours to make a "moderate" salt depletion (21). Then fluid treatment was administered based on the estimation of the deficit so as

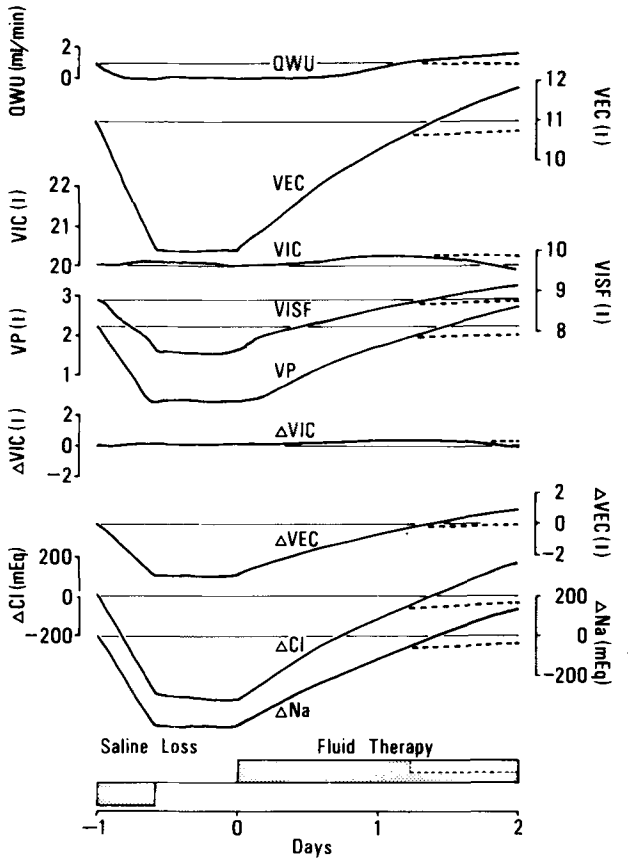

FIGURE 14. An example of simulation of isotonic saline loss and the fluid therapy. Horizontal thin line shows the normal level of each variable. After 4.5 1 of isotonic saline was pumped out of ECF in 10 hours, the amount of the deficit was calculated for water, sodium, potassium and chloride based on the result of the simulation. The fluid treatment was then started so that the deficit could be supplied in the next 48 hours, by infusing 1/2 deficit + maintenance amount. Solid lines show the changes of the variables in the simulation, and dotted lines correspond to the case in which the infusion rate was switched to the maintenance level when the urine output (QWU) returned to the normal.

to supply the total deficit in 48 hours. It is noted that the ECF volume and the amount of electrolytes rose above normal after some hours as the treatment continued (solid lines), whereas such an overshoot was avoided by switching the infusion rate to the basic allowance rate only, when the urine output (QWU) returned to normal (dotted lines). A variety of treatments could be compared through the model simulation.

We have discussed these subjects elsewhere (19), and found it very suggestive to clinicians, although confirmation of the model predictions might be rather difficult.

CONCLUSION

We have proposed a comprehensive model for the purpose of studying problems concerning body fluid disorders and fluid therapies, which includes the interactive mechanisms of circulation, renal function, body fluids, and acid-base balance. We confirmed the behavior of the model by comparing it with a number of physiological experiments, and demonstrated the possibility of applying the model to fluid therapy problems.

We consider it important that a number of different models with the same objective be proposed and compared with each other. For this purpose, some standardization of the representation and description of the models will be needed. It will be desirable that the precise description of a model is given by a set of differential equations, and also provided as a computer program coded in some programming language such as Fortran, Algol, or others suitable for scientific purposes, with the initial values for all the variables (30, 39). Symbolic expressions for mathematical formulae should be standardized. Those used in this paper (see Appendix II), seem to be a good example of simplicity and clarity.

APPENDIX I. SYMBOLS AND NORMAL VALUES

First Letter(s)		Unit
C or K	Coefficient or constant	–
PH	pH	–
F	Volume fraction	–
U	Volume content	l(STPD)/l.blood
OSM	Osmolality	mOsm/l
P	Pressure	mmHg
Q	Flow rate	l/min
R	Resistance	mmHg.min/l
V	Volume	l
MR	Metabolic production rate of gas	l(STPD)/min
T	Time constant	min
X	Concentration	mEq/l or g/dl
Y	Rate of intake or output	mEq/min
Z	Content	mEq
Exceptions: ADH, ALD, DCLA, GFR, HT, STBC, THDF, VI		

Suffix (with some exceptions)	
E	of extracellular fluid
U	of urine
I	of intracellular or input

First Letter(s)		Unit
P	of plasma	
A	of arterial vessel	
V	of venous vessel	

General abbreviations	
ECF	extracellular fluid
ICF	intracellular fluid
ISF	interstitial fluid
GFR	glomerular filtration rate

Symbol		Normal value
ADH	Effect of antidiuretic hormone (ratio to normal)	1
ALD	Effect of aldosterone (ratio to normal)	1
CFC	Capillary filtration coefficient	0.007 l/min/mmHg
CGL1	Parameter of glucose metabolism	1
CGL2	Parameter of glucose metabolism	1
CGL3	Parameter of glucose metabolism	0.03
CHEI	Transfer coefficient of hydrogen ion into ICF	5
CKAL	Weight of effect of XKE on aldosterone secretion	0.5
CNAL	Weight of effect on YNH on aldosterone secretion	0.1
CPAL	Weight of effect of PAS on aldosterone secretion	0.01
CPVL	Weight of effect of PVP on aldosterone secretion	0.1
COAD	Weight of effect of OSMP on ADH secretion	0.5
CPAD	Weight of effect of PVP on ADH secretion	1.0
CKEI	Potassium transfer coefficient from ECF to ICF	0.001
CPRX	Excretion ratio of filtered load after proximal tubule	0.2
CRAV	arterial resistance / venous resistance	5.93
CSM	Transfer coefficient of water from ECF to ICF caused by osmotic gradient	0.0003 l^2/mEq/min

Symbol		Normal value
DCLA	Chloride shift	0 mEq/l
DEN	Proportional constant between QCO and VB	1
FCOA	Volume fraction of CO_2 in dry alveolar gas	0.0561
FCOI	Volume fraction of CO_2 in dry inspired gas	0
FO2A	Volume fraction of O_2 in dry alveolar gas	0.1473
FO2I	Volume fraction of O_2 in dry inspired gas	0.21
GFR	Glomerular filtration rate	0.1 1/min
GFR0	Normal value of GFR	0.1 1/min
HF0-HF4	Parameters related to the abnormal state of the heart	0
HT	Hematocrit	45%
KL	Parameter of left heart performance	0.2
KR	Parameter of right heart performance	0.3
MRCO	Metabolic production rate of CO_2	0.2318 1(STPD)/min
MRO2	Metabolic production rate of O_2	0.2591 1(STPD)/min
OSMP	Plasma osmolality	287 mOsm/1
OSMU	Urine osmolality	461 mOsm/1
PAP	Pulmonary arterial pressure	20 mmHg
PAS	Systemic arterial pressure	100 mmHg
PBA	Barometric pressure	760 mmHg
PBL	PBA-Vapor pressure	713 mmHg
PC	Capillary pressure	17 mmHg
PCOA	CO_2 tension in alveoli	40 mmHg
PHA	pH of arterial blood	7.4
PHI	pH of intracellular fluid	7.0
PHU	pH of urine	6.0
PICO	Interstitial colloid osmotic pressure	5.0 mmHg
PIF	Interstitial fluid pressure	−6.3 mmHg
PO2A	O_2 tension in alveoli	105 mmHg
PPCO	Plasma colloid osmotic pressure	28 mmHg
PVP	Pulmonary venous pressure	4 mmHg
PVP0	Parameter of left heart performance	0 mmHg
PVS	Systemic venous pressure	3 mmHg
PVSO	Parameter of right heart performance	0 mmHg
QCFR	Capillary filtration rate	0.002 1/min
QCO	Cardiac output	5 1/min
QIC	Rate of water flow into intracellular space	0 1/min
QIN	Drinking rate	0.001 1/min

Symbol		Normal value
QIWL	Rate of insensible water loss	0.0005 1/min
QLF	Rate of lymph flow	0.02 1/min
QMWP	Rate of metabolic water production	0.0005 1/min
QVIN	Rate of intravenous water input	0 1/min
QWD	Rate of urinary excretion in distal tubule	0.01 1/min
QWU	Urine output	0.001 1/min
RTOP	Total resistance in pulmonary circulation	3 mmHg.min/1
RTOT	Total resistance in systemic circulation	20 mmHg.min/1
STBC	Standard bicarbonate at pH = 7.4	24 mEq/1
TADH	Time constant of ADH secretion	30 min
TALD	Time constant of aldosterone secretion	30 min
THDF	Effect of third factor (ratio to normal)	1
UCOA	Content of CO_2 in arterial blood	0.5612 1(STPD)/1.blood
UCOV	Content of CO_2 in venous blood	0.6075 1(STPD)/1.blood
UHB	Blood O_2 combining power	0.21.O_2 (STPD)/1.blood
UHBO	Blood oxyhemoglobin	0.21.O_2 (STPD)/1.blood
UO2A	Content of O_2 in arterial blood	0.2033 1(STPD)/1.blood
UO2V	Content of O_2 in venous blood	0.1515 1(STPD)/1.blood
VAL	Total alveolar volume	3 1
VB	Blood volume	4 1
VEC	Extracellular fluid volume	11 1
VI	Ventilation	5 1
VI0	Normal value of ventilation	5 1
VIC	Intracellular fluid volume	20 1
VIF	Interstitial fluid volume	8.8 1
VP	Plasma volume	2.2 1
VTW	Total body fluid volume	31 1
XCAE	ECF calcium concentration	5 mEq/1
XCLA	Arterial chloride concentration	104 mEq/1
XCLE	ECF chloride concentration	104 mEq/1
XCO3	ECF bicarbonate concentration	24 mEq/1
XGL0	Reference value of ECF glucose concentration	108 mg/dl
XGLE	ECF glucose concentration	6 mEq/1
XHB	Blood hemoglobin concentration	15 g/dl
XKE	ECF potassium concentration	4.5 mEq/1
XKI	ICF potassium concentration	140 mEq/1
XMGE	ECF magnesium concentration	3 mEq/1
XMNE	ECF mannitol concentration	0 mEq/1
XNE	ECF sodium concentration	140 mEq/1
XOGE	ECF organic acid concentration	6 mM/1
XPIF	Interstitial protein concentration	20 g/1

Symbol		Normal value
XPO4	ECF phosphate concentration	1.1 mM/l
XPP	Plasma protein concentration	70 g/l
XSO4	ECF sulphate concentration	1 mEq/l
XURE	ECF urea concentration	2.5 mEq/l
YCA	Renal excretion rate of calcium	0.007 mEq/min
YCAI	Intake rate of calcium	0.007 mEq/min
YCLI	Intake rate of chloride	0.1328 mEq/min
YCLU	Renal excretion rate of chloride	0.1328 mEq/min
YCO3	Renal excretion rate of bicarbonate	0.015 mEq/min
YGLI	Intake rate of glucose	0 g/min
YGLU	Renal excretion of glucose	0 mEq/min
YINS	Intake rate of insulin	0 unit/min
YKD	Rate of potassium excretion in distal tubule	0.1205 mEq/min
YKIN	Intake rate of potassium	0.047 mEq/min
YKU	Renal excretion rate of potassium	0.047 mEq/min
YMG	Renal excretion rate of magnesium	0.008 mEq/min
YMGI	Intake rate of magnesium	0.008 mEq/min
YMNI	Intake rate of mannitol	0 mEq/min
YMNU	Renal excretion rate of mannitol	0 mEq/min
YND	Rate of sodium excretion in distal tubule	1.17 mEq/min
YNH	Rate of sodium excretion in Henle loop	1.4 mEq/min
YNH0	Normal excretion rate of ammonium	0.024 mEq/min
YNH4	Renal excretion rate of ammonium	0.024 mEq/min
YNIN	Intake rate of sodium	0.12 mEq/min
YNU	Renal excretion rate of sodium	0.12 mEq/min
YOGI	Intake rate of organic acid	0.01 mM/min
YORG	Renal excretion rate of organic acid	0.01 mM/min
YPG	Flow of protein into interstitial gel	0 g/min
YPLC	Flow of protein through capillary	0.04 g/min
YPLF	Flow of protein in lymphatic vessel	0.04 g/min
YPLG	Flow of protein into pulmonary fluid	0 g/min
YPLV	Destruction rate of protein in liver	0 g/min
YPO4	Renal excretion rate of phosphate	0.025 mM/min
YPOI	Intake rate of phosphate	0.025 mM/min
YSO4	Renal excretion rate of sulphate	0.02 mEq/min
YSOI	Intake rate of sulphate	0.02 mEq/min
YTA	Renal excretion rate of titratable acid	0.0168 mEq/min
YTA0	Normal excretion rate of titratable acid	0.0068 mEq/min
YURI	Intake rate of urea	0.15 mEq/min
YURU	Renal excretion rate of urea	0.15 mEq/min
ZCAE	ECF calcium content	55 mEq
ZCLE	ECF chloride content	1144 mEq

Symbol		Normal value
ZKE	ECF potassium content	49.5 mEq
ZKI	ICF potassium content	2800 mEq
ZMGE	ECF magnesium content	33 mEq
ZMNE	ECF mannitol content	0 mEq
ZNE	ECF sodium content	1540 mEq
ZOGE	ECF organic acid content	66 mM
ZPG	Protein content in interstitial gel	20 g
ZPIF	ISF protein content	176 g
ZPLG	Protein content in pulmonary fluid	70 g
ZPO4	ECF phosphate content	12.1 mM
ZPP	Plasma protein content	154 g
ZSO4	ECF sulphate content	11 mEq
ZURE	ECF urea content	77.5 mEq

APPENDIX II. SYMBOLS FOR DRAWING THE MODEL (Figure 15)

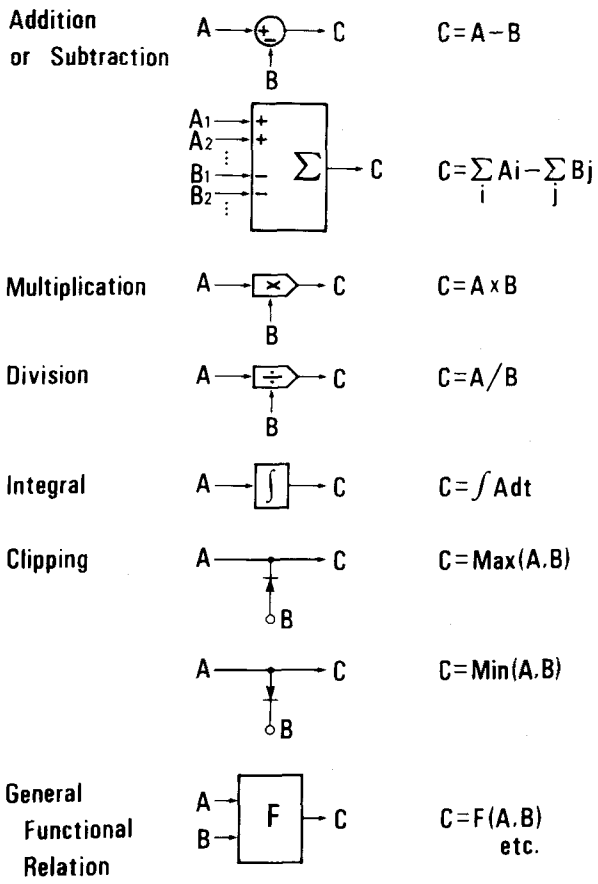

FIGURE 15. Symbols used for drawing the model.

APPENDIX III. MATHEMATICAL EXPRESSION OF FUNCTIONS

F11: Not used (see the text).

F21: $VR = k_1 [H^+] + k_2(k_3+k_4/(PO2A-32)) (PCOA+k_5) + k_6$,

where $[H^+] = 10^{9-PHA}$, $VR > 0$,

$$k_1, k_6 = \begin{cases} 0.22, -12.734 & (PHA \leqq 7.4) \\ 0.0258, -5.003 & (PHA > 7.4) \end{cases}$$

$k_3 = 0.58$, $k_4 = 3.496$,

$$k_2, k_5 = \begin{cases} 1, \ -32.08 & (PCOA > 40) \\ 0.0396, 160.11 & (PCOA \leqq 40) \end{cases}$$

F22: $PHA = 6.1 + \log (XCO3/(0.03\ PCOA))$.

F23: $UHBO = UHB \cdot f(PO2A \cdot g(PHA))$,

where $f(x) = (1-\exp(-x))^2$,

$g(x) = 0.0066815\ x^3 - 0.10098\ x^2 + 0.44921\ x - 0.454$.

F24: $XCO3 = STBC - (0.527 \cdot XHB + 3.7)(PHA - 7.4)$

$$+ 0.375\ (UHB - UHBO)/0.02226.$$

F31:

$$PIF = \begin{cases} -15 & (x \leqq 0.9) \\ 87x - 93.9 & (0.9 < x \leqq 1) \\ -6.3(2-x)^{10} & (1 < x \leqq 2) \\ x - 2 & (2 < x), \end{cases}$$

where $x = VIF/VIF_0$.

F32: $QLF = QLF_0(24/(1+\exp(-0.4977 \cdot PIF)))$.

F33: $QPLC = 2.768 \cdot 10^{-6}\ PC^2$.

F34: $PPCO = 0.4 \cdot XPP$.

F35: $PICO = 0.25 \cdot XPIF$.

F41: Rate of potassium flow into ICF (ratio to normal)

$= 1 + 0.5 \log (XKE/(56.744 - 7.06\ PHA))$.

F42: $YGLU = f_{TM}(XGLE \cdot GFR, 0.65)^*$.

F50: Effect on bicarbonate excretion $= -PCOA/120 + 4/3$.

F51:

$$YCO3 = \begin{cases} 0 & (x \leqq 2) \\ 0.1638(x-2)^{2.61} & (2 < x \leqq 4) \\ x - 3 & (4 < x), \end{cases}$$

where $x = XCO3 \cdot GFR$ F50.

F52: $YCA = f_{TM}(XCAE \cdot GFR, 0.493)^*$.

F53: $YMG = f_{TM}(XMGE \cdot GFR, 0.292)^*$.

F54: $YSO4 = f_{TM}\,(XSO4 \cdot GFR, 0.08)^*$.

F55:
$$YPO4 = \begin{cases} 5\,x/22 & (x \leqq 0.11) \\ x - 0.085 & (0.11 < x), \end{cases}$$
where $x = XPO4 \cdot GFR$.

F56:
$$YORG = \begin{cases} x/60 & (x \leqq 0.6) \\ x/3 - 0.19 & (0.6 < x), \end{cases}$$
where $x = XOGE \cdot GFR$.

F61: $YNH4 = YNH0\,(-0.5 \cdot PHU1 + 4)$.

F62: $F62 = YTA0\,(-2.5 \cdot PHA1 + 19.5)$.

F63:
$$YTA1 = \begin{cases} 0 & (PHU1 \leqq 4) \\ F62 \cdot (PHU1 - 4) & (4 < PHU1 \leqq 5) \\ F62 & (5 < PHU1). \end{cases}$$

F64: $STPO = YPO4\,(1 + 1/(1+10^{6.8-PHA}))$.

F65: Solution PHU of equation:

$$YTA = (y_p(PHA) - y_p(PHU)) + (y_o(PHA) - y_o(PHU)),$$
where $y_p(x) = YPO4(10^{-x} + 2\,10^{-6.8})/(10^{-x} + 10^{-6.8})$
and $y_o(x) = YORG \cdot 10^{-4.3}/(10^{-x} + 10^{-4.3})$.

F71: $ADH = 1.1/(1 + \exp(-0.5(ADH0 + 4.605)))$.

F72: $ALD = 10/(1 + \exp(-0.4394(ALD0 - 5)))$.

F73:
$$THDF = \begin{cases} -5.0(PPCO/28 - 1) + 1 & (PPCO \leqq 28) \\ 1 & (PPCO > 28). \end{cases}$$

F74:
$$GFR = \begin{cases} 0 & (PAS < 40) \\ 0.02\,PAS - 0.8 & (40 \leqq PAS < 80) \\ -0.005(PAS - 100)^2 + 1 & (80 \leqq PAS < 100) \\ 1 & (100 \leqq PAS). \end{cases}$$

---

*Approximated function for the Tm-limited reabsorptive mechanism:

$$f_{TM}(x,c) = \begin{cases} 0 & (x < c) \\ x - c & (c \leqq x). \end{cases}$$

REFERENCES

1. Abe, Y., F. Dixon, and J. L. McNay. Dissociation between autoregulation of renal blood flow and glomerular filtration rate. *Am. J. Physiol.* 219:986-993, 1970.
2. Blaine, E. H., J. O. Davis, and P. D. Harris. A steady-state control analysis of the renin-angiotensin-aldosterone system. *Circulation Res.* 30:713-729, 1972.

3. Brown, E. B., Jr., and B. A. Attebery. In vivo and in vitro carbon dissociation. In: *Biological Handbooks: Respiration and Circulation*, edited by P. L. Altman and D. C. Dittman. Bethesda: FASEB, 1971.
4. Burnell, J. M., M. F. Villamil, B. T. Uyeno, and B. H. Scribner. The effect in humans of extracellular pH changes on the relationships between serum potassium concentration and intracellular potassium. *J. Clin. Invest.* 35:935–939, 1956.
5. Comroe, J. H., Jr. *Physiology of Respiration*. Chicago: Year Book Medical Publishers, 1965.
6. Cunningham, D. J. C., D. J. Shaw, S. Lahiri, and B. B. Lloyd. The effect of maintained ammonium chloride acidosis on the relation between pulmonary ventilation and alveolar oxygen and carbon dioxide in man. *Q. J. Exp. Physiol.* 46:323–334, 1961.
7. Dripps, R. D., and J. H. Comroe. The effect of the inhalation of high and low oxygen concentrations on respiration, pulse rate, ballistocardiogram and arterial oxygen saturation (oximeter) of normal individuals. *Am. J. Physiol.* 149:277–291, 1947.
8. Eger, E. I., R. H. Kellog, A. H. Mines, M. Lima-Ostos, C. G. Morril, and D. W. Kent. Influence of CO_2 on ventilatory acclimatization to altitude. *J. Appl. Physiol.* 24:607–615, 1968.
9. Fujimoto, M. and T. Kubota. Role of the kidney in acid-base balance. *Sogo-Rinsho*, 24:2167–2173, 1975 (in Japanese).
10. Giebisch, G., L. Berger, and R. F. Pitts. The external response to acute acid-base disturbances of respiratory origin. *J. Clin. Invest.* 34:231–245, 1955.
11. Gray, J. S. *Pulmonary Ventilation and Its Physiological Regulation*. Springfield: Thomas, 1950.
12. Grodins, F. S. *Control Theory and Biological Systems*. New York: Columbia University Press, 1963.
13. Grodins, F. S., J. Buell, and A. J. Bart. Mathematical analysis and digital simulation of the respiratory control system. *J. Appl. Physiol.* 22:260–276, 1967.
14. Grodins, F. S., J. S. Gray, K. R. Schroeder, A. L. Norins, and R. W. Jones. Respiratory responses to CO_2 inhalation. A theoretical study of a nonlinear biological regulator. *J. Appl. Physiol.* 7:283–308, 1954.
15. Grodins, F. S., W. H. Stuart, and R. L. Veenstra. Performance characteristics of the right heart bypass preparation. *Am. J. Physiol.* 198:552–560, 1960.
16. Guyton, A. C., T. G. Coleman, and H. J. Granger. Circulation: Overall regulation. *Ann. Rev. Physiol.* 34:13–46, 1972.
17. Guyton, A. C., H. J. Granger, and A. E. Taylor. Interstitial fluid pressure. *Physiol. Rev.* 51:527–563, 1971.
18. Hirshman, C. A., R. E. McCullough, and J. V. Weil. Normal values for hypoxia and hypercapnia ventilatory drives in man. *J. Appl. Physiol.* 38:1095–1098, 1975.
19. Ikeda, N., T. Sato, H. Miyahara, F. Marumo, M. Shirataka, and H. Tsuruta. Study of fluid therapy using a model of body fluid regulation. *Proc. 21st Japanese Renal Conf.*, 263, 1978 (in Japanese).
20. Kronenberg, R., F. N. Hamilton, R. Gabel, R. Hickey, D. J. C. Read, and J. Severinghause. Comparison of three methods for quantitating respiratory response to hypoxia in man. *Respiration Physiol.* 16:109–125, 1972.
21. Marriot, H. L. Water and salt depletion. *Br. Med. J.* 1:245–250, 285–290, and 328–332, 1947.
22. Martino, J. A., and L. E. Earley. The effects of infusion of water on renal hemodynamics and the tubular reabsorption of sodium. *J. Clin. Invest.* 46:1229–1238, 1967.
23. Perez, G. O., L. Lespier, R. Knowles, J. R. Oster, and C. A. Vaamonde. Potassium homeostasis in chronic diabetes mellitus. *Arch. Internal Med.* 137:1018–1022, 1977.
24. Pitts, R. F. *Physiology of the Kidney and Body Fluids* (2nd ed.). Chicago: Year Book Medical Publishers, Inc., 1968.
25. Real, D. J. C. A clinical method for assessing the ventilatory response to carbon dioxide. *Australas. Ann. Med.* 16:20–32, 1967.
26. Rebuck, A. S., and W. E. Woodley. Ventilatory effects of hypoxia and their dependence on Pco_2. *J. Appl. Physiol.* 38:16–19, 1975.
27. Rector, F. G., Jr., D. W. Seldis, A. D. Roberts, Jr., and J. S. Smith. The role of plasma CO_2 tension and carbonic anhydrase activity in the renal reabsorption of bicarbonate. *J. Clin. Invest.* 39:1706–1721, 1960.

28. Reeve, E. B., and A. C. Guyton. *Physical Basis of Circulatory Transport*. Philadelphia: Saunders, 1967.
29. Rosenfeld, M. G. *Manual of Medical Therapeutics* (20th ed.). Waltham: Little Brown, 1971.
30. Sagawa, K. Comparative models of overall circulatory mechanics. In: *Advances in Biomedical Engineering*, edited by J. H. U. Brown and J. F. Dickson III. New York, Academic Press, 1973, vol. 3, pp. 1-92.
31. Sato, T., S. M. Yamashiro, D. Vega, and F. S. Grodins. Parameter sensitivity analysis of a network model of systemic circulatory mechanics. *Ann. Biomed. Eng.* 2:289-306, 1974.
32. Scribner, B. H. *Fluid and Electrolyte Balance*. Seattle: University of Washington, 1969.
33. Shimizu, K. Studies on osmoregulatory system: Experimental analysis with clinical and simulation studies. *Jpn. J. Nephrol.* 9:251-281, 1967 (in Japanese).
34. Swan, R. C., D. R. Axelrod, M. Seip, and R. F. Pitts. Distribution of sodium bicarbonate infused into nephrectomized dogs. *J. Clin. Invest.* 34:1795-1801, 1955.
35. Swan, R. C., and R. F. Pitts. Neutralization of infused acid by nephrectomized dogs. *J. Clin. Invest.* 34:205-212, 1955.
36. Talbot, N. B., J. D. Crawford, and A. M. Butler. Homeostatic limits to safe parenteral fluid therapy. *N. Eng. J. Med.* 248:1100-1108, 1953.
37. Taylor, A. E., W. H. Gibson, H. J. Granger, and A. C. Guyton. Review in lymphology: The interaction between intracapillary and tissue forces in the overall regulation of interstitial fluid volume. *Lymphology*, 6:192-208, 1973.
38. Woodbury, J. W. Regulation of pH. In: *Physiology and Biophysics* (19th ed.). Philadelphia: Saunders, 1965.
39. Yates, F. E. Good manners in good modeling: Mathematical models and computer simulations of physiological systems. *Am. J. Physiol.* 234:R159-160, May 1978.